Effects of starch filler on the physical properties of lyophilized calcium–alginate beads and the viability of encapsulated cells

Eng-Seng Chan [a],*, Sze-Ling Wong [a], Peh-Phong Lee [a], Jau-Shya Lee [b], Tey Beng Ti [c], Zhibing Zhang [d], Denis Poncelet [e], Pogaku Ravindra [a], Soon-Hock Phan [a], Zhi-Hui Yim [a]

[a] Centre of Materials and Minerals, School of Engineering and Information Technology, Universiti Malaysia Sabah, 88999 Kota Kinabalu, Sabah, Malaysia
[b] School of Food Science and Nutrition, Universiti Malaysia Sabah, 88999 Kota Kinabalu, Sabah, Malaysia
[c] Department of Chemical and Environmental Engineering, Faculty of Engineering, Universiti Putra Malaysia, 43400 UPM Serdang, Selangor, Malaysia
[d] Department of Chemical Engineering, University of Birmingham, Edgbaston, B15 2TT, United Kingdom
[e] ONIRIS, rue de la Géraudière, B.P. 82225-44332 NANTES Cedex 3, France

ARTICLE INFO

ABSTRACT

The main objective of this work is to improve the physical properties of lyophilized calcium (Ca)–alginate beads as a carrier material for the stabilization of encapsulated living cells. Improvements in the sphericity, flowability and mechanical strength of the dried beads were attributed to the filler, which provided structure and reinforcement to the Ca–alginate hydrogel networks, as verified by X-ray microtomography and scanning electron microscopy. A quantitative analysis of the micro-images revealed the less porous nature of the alginate–starch beads compared to the control. The beads with filler were also found to be less hygroscopic. The results also show that the cells encapsulated within the beads with reduced porosity and hygroscopicity were clearly more stable during lyophilization and storage than the control. In conclusion, the qualities of the alginate beads were improved by incorporating the solid filler, and the filler had a significant influence on cell viability during lyophilization and storage.

1. Introduction

Encapsulation is the process of confining active compounds within a matrix in particulate form to achieve certain desirable effects, such as immobilization or isolation, protection or stabilization, controlled-release, and alteration of physical properties (Chan, Lee, Ravindra, & Poncelet, 2009). Alginate is probably the most widely used material for bioencapsulation. It is a natural polysaccharide derived from marine plants, and its basic structure consists of linear unbranched polymers containing β-(1→4)-linked D-mannuronic acid (M) and α-(1→4)-linked L-guluronic acid (G) residues. Alginate forms a thermally stable and biocompatible hydrogel in the presence of di- or tri-cations. In addition, alginate beads can be easily produced by dropping an alginate solution in a calcium chloride bath. Alginate has been used in many encapsulation applications, including various fields, such as biomedical, bioprocess, pharmaceutical, food and feed. Examples of encapsulated compounds using alginate are microbial cells, herbal bioactives, and drugs, among others (Chan, Yim, Mansa, & Ravindra, 2010; Gbassi, Vandamme, Ennahar, & Marchioni, 2009; Shilpa, Agrawal, & Ray, 2003).

The critical design considerations of alginate beads are highly dependent on their intended application. The sublimation of frozen water from the alginate hydrogel matrix during the lyophilization process leaves voids within the bead structure (Sriamornsak, Thirawong, Cheewatanakornkool, Burapapadh, & Sae-Ngow, 2007; Tal, van Rijn, & Nussinovitch, 1997). As a result, the beads can develop several undesirable qualities, such as distorted shape, uneven size, poor mechanical strength and high porosity. These defective characteristics result in lesser visual appeal, and they may cause difficulty in handling. These defects may also influence the stability of the encapsulated cells during lyophilization and storage.

The main objective of this work is to improve the physical properties of lyophilized alginate beads as a carrier material for the stabilization of encapsulated living cells. Bead qualities were manipulated by incorporating a model solid filler (i.e., starch micro-granules) at various concentrations. Starch was chosen because it is readily available, cheap and edible. The first part of this work involves a characterization of the physical properties of the lyophilized alginate beads. The second part determines whether the bead properties have an influence on the stability of the encapsulated cells. The bead qualities determined were size,

* Corresponding author. Tel.: +60 88 320 000x3070; fax: +60 88 320 348.
E-mail addresses: engseng.chan@gmail.com, chan@ums.edu.my (E.-S. Chan).

size distribution, bulk and tapped densities, flowability, internal structure, pore size and porosity, mechanical properties and hygroscopicity. The beads were then used to encapsulate the model probiotic cells, *Lactobacillus casei* 01. The effects of lyophilization and storage on the viability of the encapsulated cells were determined.

2. Materials and methods

2.1. Materials

Sodium–alginate (Manugel GHB) with a medium molecular weight and high G content was supplied by ISP Technologies Inc. (Malaysia). Unmodified native corn starch (Sigma–Aldrich Inc., USA) was used as the model insoluble filler. Calcium chloride was purchased from Merck (Germany). Alginate powder and starch micro-granules were decontaminated by heat treatment in an oven at 90 °C for 15 and 30 min, respectively. This procedure avoids the hydrolysis and depolymerization of the alginate (Al-Hajry et al., 1999) as well as the gelatinization (Sajilata, Singhal, & Kulkarni, 2006) of the starch granules if an autoclave is used. This heat treatment was found to be effective, as no contamination was encountered throughout the experiments. All other solutions were sterilized using the autoclave.

2.2. Preparation of cell culture

L. casei 01 (Chr. Hansen, Malaysia) was used as the model cells. The cells were grown at 37 °C in an MRS broth (Oxoid, UK), and they were grown and transferred three times before use. The cells were harvested by centrifugation when their growth reached the stationary phase. They were washed three times with saline (8.5 g/L of NaCl) to remove any nutrients carried from the MRS broth.

2.3. Preparation of beads used for encapsulating cells

The cell suspension was mixed to a solution containing 20 g/L of alginate and 0–600 g/L of starch. The solution was extruded through a capillary and dropped into a calcium chloride (15 g/L) bath for gelation. The beads were hardened for 30 min before being rinsed with distilled water. The beads were then lyophilized at −55 °C and 10^{-2} mbar for 24 h. Capillary tips with diameters ranging from 0.55 to 1.65 mm were used to adjust the bead diameter to approximately 2 mm after lyophilization.

2.4. Determination of liquid properties

The densities of the alginate-filler solutions were measured with a digital densitometer (Kyoto Electronics Manufacturing Co. Ltd., Japan). The viscosity was determined by a viscometer according to a standard procedure (Brookfield Engineering Laboratories, Inc., Model: LV-DV E203, USA). The surface tension of the alginate solution at 20 g/L was obtained from Chan et al. (2009), and it was assumed to be constant with different starch concentrations. All measurements were performed at a room temperature of 24 ± 1 °C.

2.5. Determination and calculation of alginate drop/bead size

The bead size was determined using image analyzer software (SigmaScan Pro 5, SPSS Inc.). The diameters of the beads obtained experimentally before lyophilization was compared to those obtained from calculation. The diameters of the alginate liquid drops were calculated from an equation based on Tate's, which was corrected using a set of correction factors to estimate the diameter of the Ca–alginate beads after gelation (Chan et al., 2009). These factors are expressed as follows:

Theoretical diameter of detached liquid drop, $D_{l(T)}$ (mm):

$$D_{l(T)} = \left(\frac{6 d_T \gamma}{\rho g} \right)^{1/3} \tag{1}$$

where d_T is the capillary tip diameter (mm); γ is surface tension (g/s^2); ρ is density (g/mm^3); and g is gravitational force (mm/s^2).

Corrected diameter of detached liquid drop, $D_{l(C)}$ (mm):

$$D_{l(C)} = k_{LF} \times D_{l(T)} \tag{2}$$

where k_{LF} is the liquid lost factor, $k_{LF} = 0.98 - 0.04 d_T$.

Corrected diameter of Ca–alginate bead after gelation, $D_{b(C)}$ (mm):

$$D_{b(C)} = k_{SF(gelation)} \times D_{l(C)} \tag{3}$$

where k_{SF} is the shrinkage factor attributed to the gelation process, which was found to be $k_{SF(gelation)} = 0.88$ (Chan et al., 2009).

The reduction in bead size after lyophilization was calculated and expressed by a shrinkage factor, as shown below:

$$k_{SF(lyophilization)} = \frac{D_b - D_{b(lyophilized)}}{D_b} \tag{4}$$

where $k_{SF(lyophilization)}$ is the shrinkage factor attributed to the lyophilization process; D_b is the diameter of the bead obtained experimentally before lyophilization (mm); and $D_{b(lyophilized)}$ is the diameter of the bead obtained experimentally after lyophilization (mm).

2.6. Determination of bead shape

The bead shape was quantified using the sphericity factor (SF), which is given by the following equation:

$$\text{Sphericity factor (SF)} = \frac{d_{max} - d_{min}}{d_{max} + d_{min}} \tag{5}$$

where d_{max} is the largest diameter and d_{min} is the smallest diameter perpendicular to d_{max}.

The d_{max} and d_{min} were measured using image analyzer software, and the sphericity factor was computed using Microsoft Excel.

2.7. Determination of bulk density, tapped density and flowability

The bulk density (ρ_{BD}) of the lyophilized beads was determined by pouring a known mass of beads (m_p) into a measuring cylinder, and it was calculated by dividing the mass (m_p) by the bulk volume (v_B) (Abdullah & Geldart, 1999), as shown in following equation:

$$\rho_{BD} = \frac{m_P}{v_B} \tag{6}$$

The tapped density (ρ_{TD}) was determined using a tap density analyzer. A measuring cylinder containing beads was tapped until the equilibrium tap volume (v_T) was obtained. The flowability of the beads was indicated by the Hausner ratio, which can be calculated according to the following equation (Kumar, Kothari, & Banker, 2001):

$$\text{Hausner ratio} = \frac{\rho_{TD}}{\rho_{BD}} \tag{7}$$

2.8. Imaging of internal structure

The internal structure of the lyophilized beads was examined using a scanning electron microscope (SEM; JEOL JSM-5610LV, Japan). Prior to scanning, the beads were cut through the center to expose a cross-section, and they were gold-plated with a sputter coater (JEOL JFC-1600, Japan). In addition, X-ray microtomography

(SkyScan 1072, Belgium) was used to visualize the internal structure without any treatment to the beads.

2.9. Porosity and pore size analysis

The beads' cross-sectional images acquired from the X-ray microtomography were analyzed using TView software (SkyScan, Belgium) to determine the relative porosity (%). The pore size was measured with a mercury porosimeter (Thermo Electron, Pascal 440, Italy) with pressures ranging from 0 to 200 MPa.

2.10. Determination of mechanical strength

The mechanical strength of single lyophilized beads was qualitatively determined using a texture analyzer (Hounsfield H1KF, UK). Single lyophilized beads were positioned on a flat platform and were compressed in a vertical direction using a flat-tip probe, which was connected to a force transducer. The forces imposed on the beads and the displacement was recorded during compression.

2.11. Determination of hygroscopicity

The hygroscopicity of the lyophilized beads was evaluated based on the equilibrium of moisture content achieved when exposed to 80% relative humidity at 30 °C in a closed container. A saturated ammonium sulfate solution (Fluka, Switzerland) was used to control the relative humidity. The moisture content of the samples was measured gravimetrically at the desired time intervals. The moisture content was expressed as percentage in dry weight (% d.w.).

2.12. Determination of cell stability

The encapsulated cells were released by dissolving the Ca–alginate beads in a sodium citrate solution (40 g/L) (Riedel-de Haën, Germany), and they were homogenized using a stomacher. The cell suspension was serially diluted in an MRD solution (Oxoid, UK) and was spread onto pre-dried MRS agar (Oxoid, UK). The number of colonies formed on the plates was counted after incubation for two days at 37 °C. The cell viability was taken before and after the drying process to determine the cell stability during lyophilization. For cell stability during storage, the cell viability was determined periodically. The storage temperature was set at 30 °C, and the relative humidity was fixed at 44% using a saturated potassium carbonate solution (Riedel-de Haën, Germany). The D-value was used to describe the duration required to reduce the cell viability by 90% under the storage condition.

2.13. Statistical analysis and control

Thirty beads were used for each analysis. The measurements were repeated at least twice to determine the mean and the standard error. The Ca–alginate beads without starch (i.e., 0 g/L filler concentration) were taken as the control.

3. Results and discussion

3.1. Bead size

As apparent in Fig. 1a, the alginate drop size decreased systematically along the process of dripping, gelation and lyophilization. By using the extrusion-dripping technique, an alginate liquid pendant drop grew at the capillary tip until the surface tension force no longer supported the weight of the drop. At this instant, the liquid drop detached from the tip and fell into the gelling bath to form a bead. Tate's law, which approximates the balance between
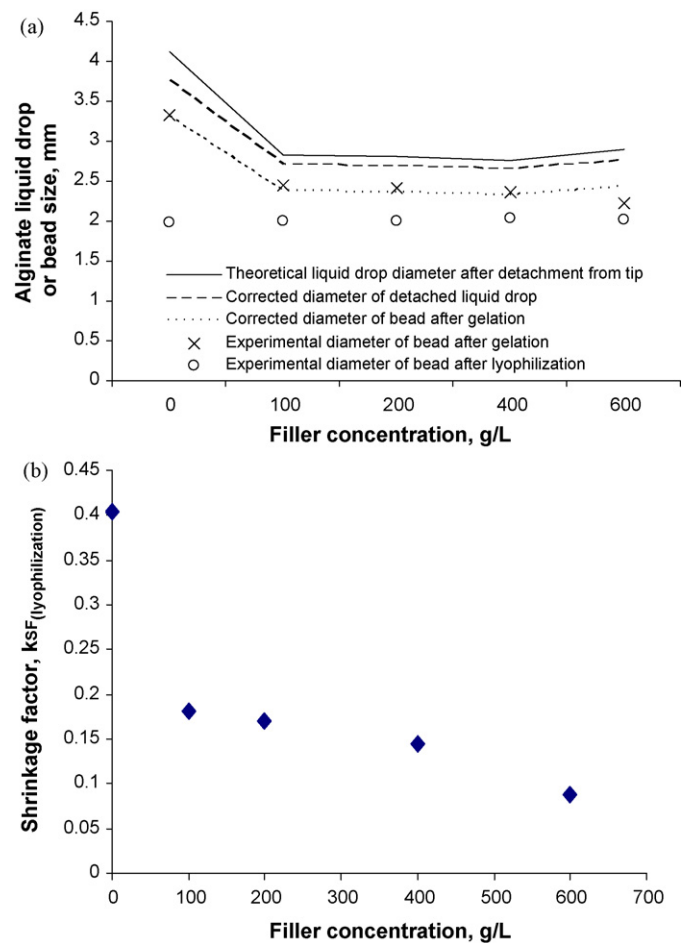

Fig. 1. (a) Evolution of alginate drop size along the encapsulation and lyophilization process and (b) effect of filler concentration on shrinkage of lyophilized Ca–alginate bead.

the gravitational force pulling the drop down and the surface tension force holding the drop pendant to the tip at the instant of drop detachment, can be used to predict the theoretical size of the detached liquid drop. However, it is well known that a small fraction of liquid pendant drop will remain undetached at the tip when the main drop breaks away from the tip. To take this effect into account, the theoretical liquid drop size can be corrected using the liquid lost factor (k_{LF}) (Chan et al., 2009), as shown in Table 1. The liquid lost factor (k_{LF}) was found to be independent of the liquid's properties but was dependent on the tip size.

When the liquid drop fell into the gelling bath to form a bead, the bead size was found to be smaller than the liquid drop. This phenomenon has been attributed to the syneresis effect during the gelation process, and the bead size can be corrected using the shrinkage factor, $k_{SF(gelation)}$ (Chan et al., 2009), as shown in Table 1. The shrinkage factor was found to be mainly influenced by the M/G ratio of the alginate. The bead diameter after gelation, calculated using the correction factors (i.e., k_{LF} and $k_{SF(gelation)}$), was found to give a close estimation to that obtained experimentally, with an average absolute deviation (AAD) of less than 3%. This indicates that the validity of the size prediction model was not influenced by the presence of the filler material.

The lyophilization process was found to cause further reduction in bead size. The degree of shrinkage was dependent on the starch concentration (see Fig. 1b). The control bead (i.e., without filler) shrunk the most, by about 40% (i.e., $k_{SF(lyophilization)} = 0.6$). As shown in Fig. 1b, the addition of filler reduced the shrinkage

Table 1
Estimation of bead size before lyophilization.

Filler conc. (g/L)	Tip diameter d_T (mm)	Density ρ (g/cm^3)	Viscosity η (cP)	Surface tension (g/s^2)[a]	Theoretical diameter of detached liquid drop $D_{l(T)}$ (mm)	Corrected diameter of detached liquid drop $D_{l(C)}$ (mm)	Corrected diameter of bead after gelation $D_{b(C)}$ (mm)
0	1.65	1.01	283.63		4.12	3.77	3.32
100	0.55	1.04	333.90		2.83	2.71	2.39
200	0.55	1.07	398.90	70	2.80	2.69	2.36
400	0.55	1.11	811.90		2.77	2.65	2.33
600	0.65	1.15	1890.00		2.89	2.76	2.43

[a] Obtained from Chan et al. (2009).

significantly as the beads with increasing starch concentrations (100–600 g/L) shrank from 18 to 9%. This shows that the addition of the insoluble filler can effectively control the degree of shrinkage. This observation is consistent with previous works (Rassis, Saguy, & Nussinovitch, 2002; Zohar-Perez, Chet, & Nussinovitch, 2004). In this study, the bead diameter after lyophilization was maintained at about 2 mm by using dripping tips with different diameters to ensure that the bead size after lyophilization did not become a variable in subsequent studies.

3.2. Shape and surface texture

The shape of the alginate beads was represented using the sphericity factor because it can detect the shape change more efficiently than other dimensionless shape indicators, such as circularity and aspect ratio. The sphericity factor varies from zero for a perfect sphere to approaching unity for an elongated object. Fig. 2 shows the shapes of lyophilized beads at different filler concentrations. Before lyophilization, the shapes of all the beads were spherical regardless of the filler concentration. After lyophilization, the shapes of the control beads were irregular, but the shapes of the beads with filler remained spherical.

The shape of the Ca–alginate beads produced using the extrusion-dripping method was mainly influenced by the liquid properties (i.e., surface tension and viscosity of the alginate and gelling solutions) and the process conditions (i.e., collecting distance). In our recent study, it was found that the critical Ohnersorge number $Oh = \eta/(\rho d_p \gamma)^{1/2}$ of an alginate liquid drop is approximately 0.24. Below this number, spherical Ca–alginate beads could not form (Chan et al., 2009). In this study, the Ohnersorge numbers ranged from 0.57 to 4.3 for filler concentrations of 0 g/L to 600 g/L, and they were all above the critical value. In addition, the optimum collecting distance was determined to produce spherical beads. The distance ranged from 3 to 35 cm depending on the filler concentrations, which ranged between the 'minimum collecting distance,' below which a bead with a distinct tail is produced, and the 'maximum collecting distance,' above which shape deformation occurs.

Fig. 2 shows that the lyophilization process caused the structure of the control beads to collapse when water was sublimated from the hydrogel matrix. This collapse resulted in beads with an irregular shape, a phenomenon that was also observed in previous works (Rassis et al., 2002; Zohar-Perez et al., 2004). However, the addition of filler, even at a low concentration (i.e. 100 g/L) was enough to maintain the beads' sphericity during lyophilization. Increasing the filler concentration did not show further improvement in bead sphericity. This suggests that the filler was able to act as a structural support to control the size of shrinkage and to maintain the shape of the hydrogel material during drying. A similar finding was reported using other non-soluble fillers, such as kaolin, bentonite, ceramic powders and rice starch (Ribeiro, Barrias, & Barbosa, 2004; Zohar-Perez et al., 2004).

The appearance of the lyophilized beads was also examined visually. As expected, the control beads were light brown in color,

whereas the addition of filler (i.e., starch micro-granules) made the beads white in color. In addition, the lyophilization process had an obvious effect on the beads' surface morphology. The sublimation of the water crystals not only caused shrinkage of the hydrogel matrices but also left voids. This resulted in uneven, porous and rough surfaces, as shown by the control beads. In contrast, the addition of filler produced beads with smooth and even surfaces. Despite this observation, it was found that the surface morphological qualities also depend on the filler's properties. According to Rassis et al. (2002) and Zohar-Perez et al. (2004), a filler with a smaller particle size gives a smoother surface.

3.3. Bulk, tapped density and flowability of beads

Bulk density can be defined as the mass of beads divided by the total volume they 'freely' occupy, which includes the bead volume, the inter-particle void volume and the internal pore volume. Tapped density refers to the bulk density of the beads after a specified compaction process, which usually involves vibrating or tapping the container. In this study, it was found that the densities increased with increasing filler concentration, and the tapped density was found to be higher than the bulk density (figure not shown).

The Hausner ratio of a granular material is a measure of the inter-particle friction or cohesiveness of the material (Abdullah & Geldart, 1999). This ratio can be used to describe the degree of compaction of the beads, and it can be defined as the ratio of the tapped density to the bulk density, as expressed by Eq. (4). A larger value indicates greater inter-particle friction. The friction is basically affected by the type of material, the bead shape and size, the surface conditions, the size distribution, the atmospheric conditions (humidity and temperature) and the inter-particle forces (i.e., cohesion and electrostatics). A Hausner ratio of less than 1.25 has been used to indicate good flowability (Rough, Wilson, Bayly, & York, 2003) since particles at this ratio show little potential for further consolidation (Anderson, Cheng, & Nacht, 1994).

In this study, all lyophilized beads were free flowing, as observed visually and as indicated by Hausner ratios less than 1.25 (figure not shown). Despite this quality, the control beads had the highest ratio (i.e., 1.10). This high ratio could be due to the irregular shape and rough surface of these beads, which increased inter-particle friction. This effect of bead shape on the Haunsner ratio was also observed by Abdullah and Geldart (1999). However, the Haunsner ratios of the beads with various filler concentrations were relatively similar. This similarity could be attributed to the uniform bead size and size distribution and their smooth surface. In brief, the density of the lyophilized Ca–alginate beads can be adjusted by the addition of filler material, and the addition of filler improves the flowing property of the beads.

3.4. Internal structure

X-ray microtomography was used to visualize the internal structure of the beads. This imaging technique is non-destructive,
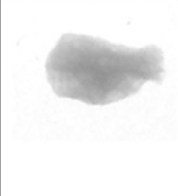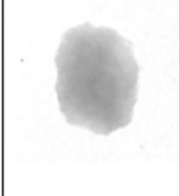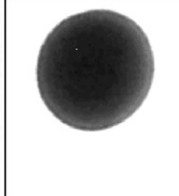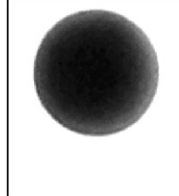
Filler concentration (g/L)	0	0	100	600
Image				
Sphericity factor (SF)	0.285	0.152	0.041	0

Fig. 2. Shape of beads after lyophilization at different filler concentrations.

and it combines X-ray microscopy with tomographical algorithms that generate 3D images of a sample's morphology and internal structure. When there are differences in the density of a sample, variations in the X-ray's attenuation (i.e., absorption and scattering) produce a contrast in the image. As shown in Fig. 3a1–a3, the white areas correspond to the Ca–alginate matrices and starch micro-granules, and the black areas represent the voids. The control bead (Fig. 3a1) has a macroporous internal contour structure in which the hydrogel matrices form dense concentric layers at the surface with voids between the matrices. This observation is verified by the SEM micrograph (Fig. 3b1) and by previous studies (Rastello De Boisseson et al., 2004; Nussinovitch & Zvitov-Marabi, 2008). The contour structure is associated with the cross-linking direction of the external gelation process, where gelation occurs radially from the surface toward the inner core of the bead. The homogeneity of the internal structure of a Ca–alginate bead can be controlled during the bead's formation process by adding competing ions (i.e., sodium chloride) to the gelling solution (Skjåk-Bræk, Grasdalen, & Smidsrød, 1989) or by using a modified emulsifica-

tion method (Fundueanu, Nastruzzi, Carpov, Desbrieres, & Rinaudo, 1999).

When the filler was added at a low concentration (100 g/L), the internal structure of the bead was less porous because the filler occupied the interstitial spaces between the concentric layers (see Fig. 3a2 and b2). The X-ray imaging also reveals a 'spider-web' pattern in which the filler forms 'bridges' that connect the concentric layers. This was also observed by Tal et al. (1997). The filler gives structural support to the gel network and prevents structural collapse or shrinkage during lyophilization. In addition, the X-ray images show that the filler's spatial distribution within the beads is uneven at low concentration. At 200 g/L (figure not shown), the concentration of filler is higher around the inner core than near the bead surface. The tendency to fill the inner core could be due to the cavity at the center being larger than near the surface. This tendency was attributed to the direction of the cross-linking process, as mentioned earlier, which forms denser gel layers and, thus, less 'readily available space' at the surface compared to the inner core. When the filler concentration was increased to 600 g/L, the addi-
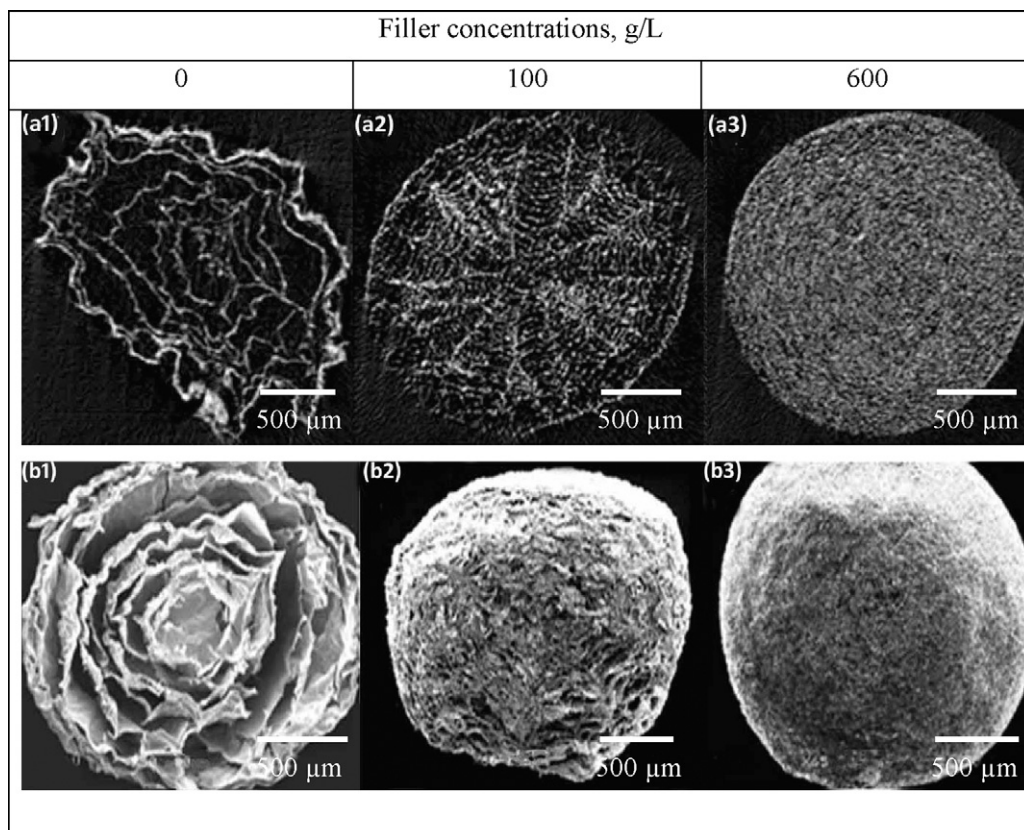

Fig. 3. (a1–3) X-ray microtomography and (b1–3) scanning electron microscopy images of lyophilized alginate beads at different filler concentrations.
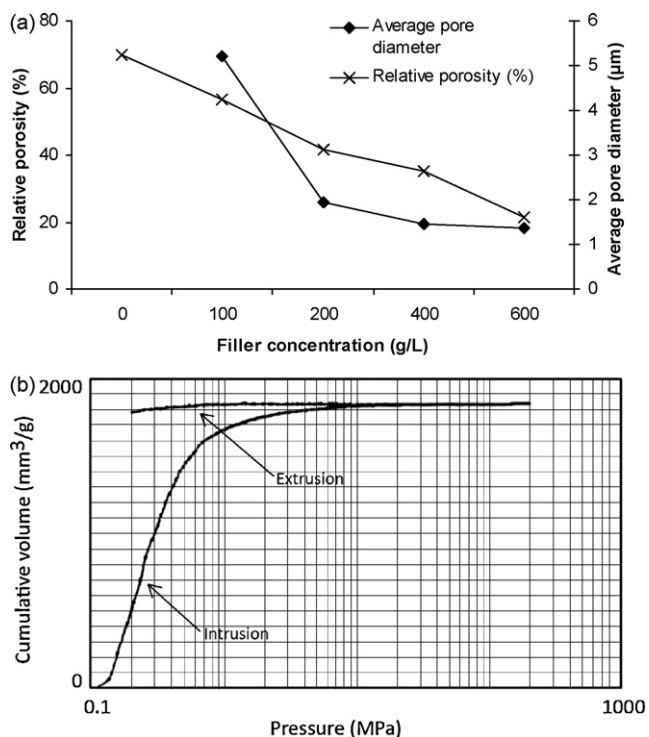
Fig. 4. Pore analysis of lyophilized beads: (a) relative porosity and pore diameter and (b) pore shape.

tional filler was forced to fill the remaining space, which resulted in a more uniform spatial distribution of filler within the bead, as shown in Fig. 3a3 and b3.

3.5. Porosity and pore size analysis

The relative porosity (%) of the beads was determined by analyzing the X-ray images. It was found that the relative porosity declined linearly with increasing filler concentration, and the control beads were three times more porous than those with a filler concentration of 600 g/L (Fig. 4a). When the pore size was determined using a mercury porosimeter, it was found that the pore sizes reduced with increasing filler concentration. This observation is in good agreement with Tal et al. (1997). In general, the lyophilized beads can be categorized as macroporous material since their pore diameters are larger than 0.1 μm according to the IUPAC definitions (Ferrero & Jiménez-Castellanos, 2002).

The intrusion–extrusion curves from the mercury porosimetry technique may be used to indicate the pore shape of the lyophilized bead, as shown in Fig. 4b. An intrusion curve is a volume–pressure curve with increasing pressure, whereas an extrusion curve is a volume–pressure curve with decreasing pressure. In general, the pore shape can be divided into three different types: cylindrical, conical and ink-bottle. These three shapes depend on the pattern of the intrusion–extrusion curve. The intrusion–extrusion curve of the lyophilized Ca–alginate-filler beads is shown in Fig. 4b. It shows a characteristic ink-bottle shape, which can be described as a larger central cavity linked to a surface by smaller-diameter capillaries (Emeruwa, Jarrige, & Mexmain, 1991). The low penetration pressure of the beads indicates the presence of macro-pores.

3.6. Mechanical properties of beads

Fig. 5 shows the force–strain relationship of the lyophilized beads. The addition of filler increased the rigidity of the beads. This increased rigidity is indicated by the higher force imposed on the
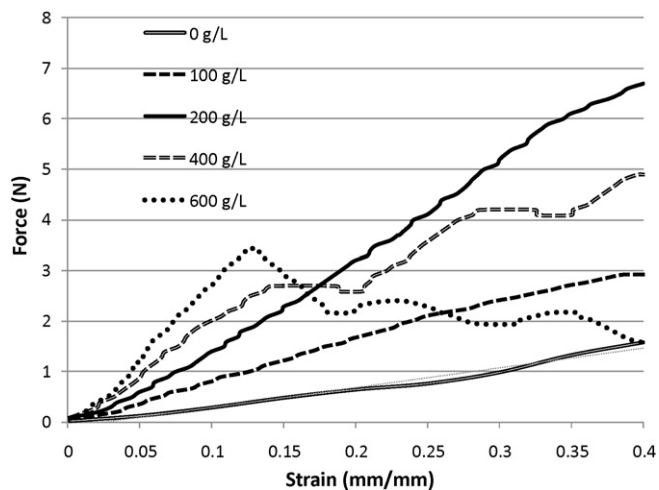

Fig. 5. Force–strain curves of lyophilized Ca–alginate beads at different filler concentrations.

bead at a specific strain compared to that of the control beads (see Fig. 5). The control beads and the beads at low filler concentrations (i.e., less than 200 g/L) were spongy, as they were elastic even after deformation at 40% strain. However, as the beads became more brittle, they cracked at lower strains at higher filler concentrations (i.e., more than 200 g/L). This activity is clearly shown by the presence of breakage points in the force–strain curves of the beads with filler concentrations of 400 g/L and 600 g/L.

From our prior experience, the quality of lyophilized Ca–alginate beads can be either spongy and not friable or fragile and friable. The reason for the variation in the physical characteristics is not clear, but it could be due to the lyophilization conditions or the amount of residual water within the beads after the lyophilization process. If the beads are fragile and friable, they can cause problems in handling and further processing since they can easily break and disintegrate. The addition of filler was found to avoid these problems, as the beads were rigid and not friable. These characteristics are due to the filler reinforcing the hydrogel network and filling the voids, as shown by the X-ray and SEM images (Fig. 3). However, the increase in filler concentration led to fewer voids and denser packing. As a result, the beads lost their flexibility, and they became brittle.

3.7. Hygroscopicity

Hygroscopicity is used to describe how readily a material absorbs moisture from the atmosphere. It is well known that lyophilized materials are highly sensitive to humidity. This sensitivity can result in a rapid loss of cell viability when stored under unfavorable conditions. In this work, the hygroscopicity was quantified by determining the moisture sorption kinetics of the lyophilized beads, as shown in Fig. 6. The control beads were found to be the most hygroscopic, as they had the highest moisture absorption rates and the highest water content at equilibrium. However, the addition of filler was generally found to lower the moisture absorption rate and the equilibrium water content.

The hygroscopicity of the control beads could be due to the hydrophilic nature of alginate (Rhim, 2004; Olivas & Barbosa-Cánovas, 2008). However, the addition of starch granules was found to reduce bead hygroscopicity. This change in hygroscopicity could be due to the chemical property of the starch granules, which is formed by layers of amorphous and crystalline regions. The amorphous region is mainly amylose and the crystalline region is primarily amylopectin, which is believed to be vapor-resistant (Gorrasi et al., 2008). Starch granules may also contain a small
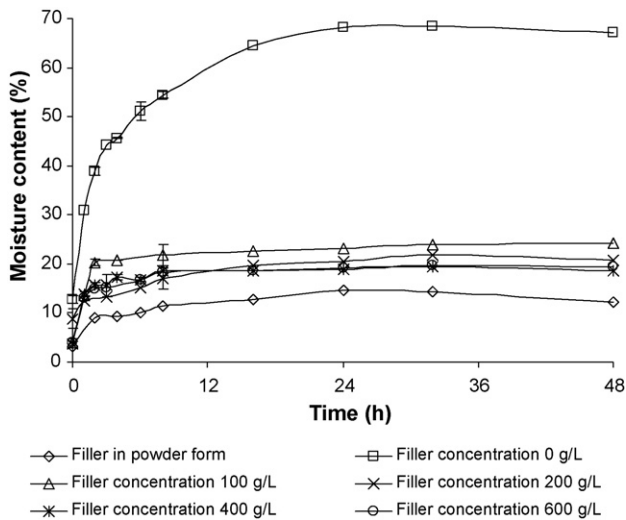
Fig. 6. Moisture sorption curves of the lyophilized beads. Exposure conditions: 80% relative humidity at 30 °C. The error bars indicate the standard error of the samples.

amount of lipids, which can also suppress the moisture sorption rate of the beads.

3.8. Stability of encapsulated cells

During hydrogel bead production, the encapsulation efficiency was found to be close to 100%. The encapsulation efficiency was calculated based on the ratio of viable cells after encapsulation over the initial number of viable cells. The efficiency was high because the cells measured about 1–10 μm, whereas the estimated pore size of the Ca–alginate hydrogel was reported to be less than 17 nm (Krasaekoopt, Bhandari, & Deeth, 2004). The addition of filler was found to have no influence on the encapsulation efficiency. The stability of the encapsulated cells after lyophilization and storage was then studied.

After lyophilization, the cells encapsulated in the control beads were found to have the lowest survival rate (lost of 4 log, see Fig. 7a). In comparison, the survival of cells encapsulated within the beads with filler was 100 times higher (1.5–2 log lost of viable cells). Lyophilization is a widely used dehydration method for cell preservation. There have been a number of reports regarding the adverse effects of lyophilization on cellular structure and cell functions, which can eventually lead to the loss of cell viability (Chan & Zhang, 2002, 2005; De Giulio et al., 2005). Among the effects reported are protein denaturation and damage to the cell wall and cell membrane. Champagne et al. (1992) found that the Ca–alginate hydrogel matrix alone did not protect the encapsulated cells. This finding is in good agreement with the present work. In fact, the cell survival was found to be similar to that of the non-encapsulated cells (data not shown).

The difference in the survival of cells encapsulated in Ca–alginate beads with and without filler when lyophilized might be attributable to the physical properties of the beads. Since the degree of shrinkage of the control beads was higher, it could cause more physical stress to the cells during lyophilization. Moreover, the highly porous nature of the control beads had more surface area in which the cells could be directly exposed to lyophilization. This exposure could decrease cell survival since it is reported that the probability of death during lyophilization is proportional to the exposed surface area (Bozoğlu, Özilgen, & Bakir, 1987). However, the addition of filler not only reduced shrinkage, it offered physical protection to the cells by shielding them against the detrimental effect of lyophilization through a densely packed environment.
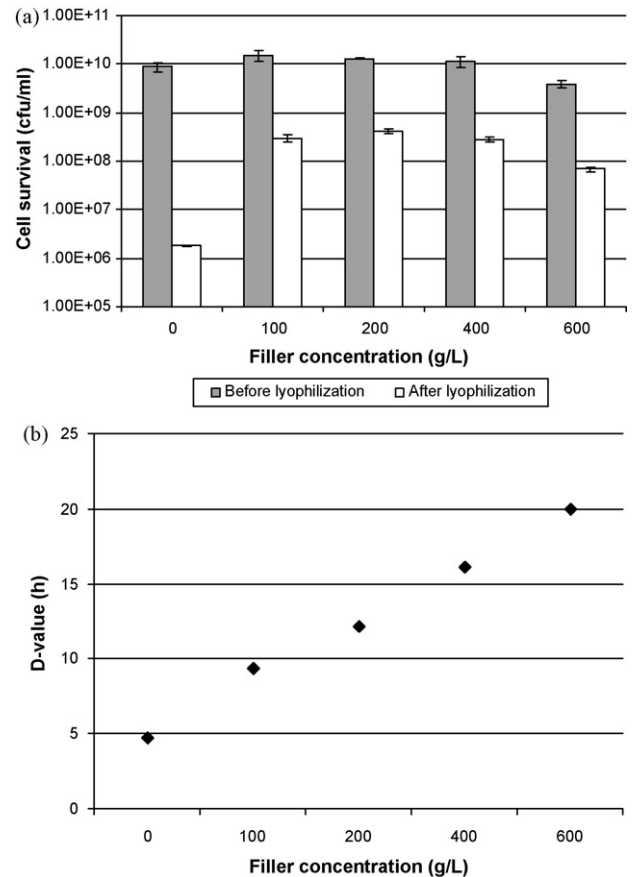
Fig. 7. Effect of filler on (a) the survival of encapsulated cells when subjected to lyophilization and (b) the cell stability during storage at 30 °C and 44% relative humidity.

The stability of encapsulated cells during storage was subsequently studied. The cell survival is expressed by the D-value (i.e., decimal reduction time), which is defined as the time needed for the number of viable cells to decrease tenfold. The cell viability was periodically monitored during exposure to a closed controlled environment of 44% relative humidity at 30 °C. The results clearly show that the cells were more stable when encapsulated within the beads with filler (see Fig. 7b). The cell stability also increased with higher filler concentrations. The storage stability of beads with a filler concentration of 600 g/L was found to be 4 times higher than that within the control beads.

Several earlier works have found that storage conditions and additive formulation (e.g., addition of cryoprotectant) have a significant effect on cell stability during storage. In general, a higher temperature and relative humidity result in lower cell stability because various biochemical reactions, such as lipid oxidation and enzymatic reactions, can be accelerated (Champagne, Mondou, Raymond, & Roy, 1996; Ishibashi, Tatematsu, Shimamura, Tomita, & Okonogi, 1985). Also, it has been speculated that the presence of oxygen can lead to oxidation reactions that cause protein denaturation and phospholipid degradation of dried biological materials (Castro, Teixeira, & Kirby, 1996; Greiff, 1971). However, various types of additives, such as trehalose, sucrose, gelatin and skimmed milk, have been added to improve cell stability during storage (Andersen, Fog-Petersen, Larsen, & Skibsted, 1999; Schebor, Burin, Pilar Buera, & Chirife, 1999).

In this study, additives were not used so that the effects of bead properties on cell stability could be clearly observed. It is evident that the bead properties have a significant influence on cell stability during storage. The lower stability of cells encapsu-

lated within the control beads could be due to the highly porous nature and distorted shape of the beads. These undesirable bead qualities can increase the surface areas that are directly exposed to environmental stress factors such as oxygen, moisture, heat and radiation. In contrast, the stability of the cells encapsulated within the beads with filler was higher because the bead porosity was lower. These characteristics provided a densely packed environment that effectively shielded the cells from the stress factors. The lower hygroscopicity of the alginate-filler beads also resulted in higher cell stability during storage.

4. Conclusions

This study describes the effects of a model insoluble filler material (starch micro-granules) on the physical properties of lyophilized calcium–alginate beads and the viability of encapsulated cells. The addition of filler was found to improve the sphericity, flowability, density, visual quality and rigidity of the beads, which are desirable qualities for processing, handling and consumer usage. These characteristics resulted from the filler's ability to reinforce the hydrogel network and fill the interstitial voids. In addition, the viability of encapsulated living cells was found to be closely associated to the bead properties. The beads that were less porous and less hygroscopic resulted in higher cell viability when lyophilized and during storage. Future works may involve the use of other solid fillers such as microcrystalline cellulose, resistant starch or insoluble dietary fiber (e.g. prebiotics) to create additional functionalities to the encapsulated cell system.

Acknowledgment

References

Abdullah, E. C., & Geldart, D. (1999). The use of bulk density measurements as flowability indicators. *Powder Technology*, 102(2), 151–165.
Al-Hajry, H. A., Al-Maskry, S. A., Al-Kharousi, L. A., El-Mardi, O., Shayya, W. H., & Goosen, M. F. A. (1999). Electrostatic encapsulation and growth of plant cell cultures in alginate. *Biotechnology Progress*, 15, 768–774.
Andersen, A. B., Fog-Petersen, M. S., Larsen, H., & Skibsted, L. H. (1999). Storage stability of freeze-dried starter cultures (*Streptococcus thermophilus*) as related to physical state of freezing matrix. *Food Science and Technology*, 32, 540–547.
Anderson, D. L., Cheng, C., & Nacht, S. (1994). Flow characteristics of loosely compacted macroporous microsponge® polymeric systems. *Powder Technology*, 78, 15–18.
Bozoğlu, T. F., Özilgen, M., & Bakir, U. (1987). Survival kinetics of lactic acid starter cultures during and after freeze-drying. *Enzyme and Microbial Technology*, 9, 531–537.
Castro, H. P., Teixeira, P. M., & Kirby, R. (1996). Changes in the cell membrane of *Lactobacillus bulgaricus* during storage following freeze-drying. *Biotechnology Letters*, 18(1), 99–104.
Champagne, C. P., Mondou, F., Raymond, Y., & Roy, D. (1996). Effect of polymers and storage temperature on the stability of freeze-dried lactic acid bacteria. *Food Research International*, 29(5), 555–562.
Champagne, C. P., Morin, N., Couture, R., Gagnon, C., Jelen, P., & Lacroix, C. (1992). The potential of immobilized cell technology to produce freeze-dried, phage-protected cultures of *Lactococcus lactis*. *Food Research International*, 25(6), 419–427.
Chan, E.-S., Lee, B.-B., Ravindra, P., & Poncelet, D. (2009). Prediction models for shape and size of calcium–alginate macrobeads produced through extrusion technique. *Journal of Colloid and Interface Science*, 338, 63–72.

Chan, E.-S., Yim, Z.-H., Mansa, R. F., & Ravindra, P. (2010). Encapsulation of herbal aqueous extract through absorption with Ca–alginate hydrogel beads. *Food and Bioproducts Processing*, 88, 195–201.
Chan, E.-S., & Zhang, Z. (2002). Encapsulation of probiotic bacteria *Lactobacillus acidophilus* by direct compression. *Food Bioproducts Process*, 80, 78–82.
Chan, E.-S., & Zhang, Z. (2005). Bioencapsulation by compression coating of probiotic bacteria for their protection in an acidic medium. *Process Biochemistry*, 10, 3346–3351.
De Giulio, B., Orlando, P., Barba, G., Coppola, R., De Rosa, M., Sada, A., et al. (2005). Use of alginate and cryo-protective sugars to improve the viability of lactic acid bacteria after freezing and freeze-drying. *World Journal of Microbiology and Biotechnology*, 21, 739–746.
Emeruwa, E., Jarrige, J., & Mexmain, J. (1991). Application of mercury porosimetry to powder (UO₂) analysis. *Journal of Nuclear Materials*, 184, 53–58.
Ferrero, C., & Jiménez-Castellanos, M. R. (2002). The influence of carbohydrate nature and drying methods on the compaction properties and pore structure of new methyl methacrylate copolymers. *International Journal of Pharmaceutics*, 248, 157–171.
Fundueanu, G., Nastruzzi, C., Carpov, A., Desbrieres, J., & Rinaudo, M. (1999). Physico-chemical characterization of Ca–alginate microparticles produced with different methods. *Biomaterials*, 20, 1427–1435.
Gbassi, G. K., Vandamme, T., Ennahar, S., & Marchioni, E. (2009). Microencapsulation of *Lactobacillus plantarum* spp in an alginate matrix coated with whey proteins. *International Journal of Food Microbiology*, 129, 103–105.
Gorrasi, G., Vittoria, V., Murariu, M., Ferreira, A. D. S., Alexandre, M., & Dubois, P. (2008). Effect of filler content and size on transport properties of water vapor in PLA/calcium sulfate composites. *Biomacromolecules*, 9(3), 984–990.
Greiff, D. (1971). Protein structure and freeze-drying: The effects of residual moisture content and gases. *Cryobiology*, 8, 145–152.
Ishibashi, N., Tatematsu, T., Shimamura, S., Tomita, M., & Okonogi, S. (1985). Effect of water activity on the viability of freeze-dried bifidobacteria and lactic acid bacteria. *International Institute of Refrigeration, Paris*, 227–232.
Krasaekoopt, W., Bhandari, B., & Deeth, H. C. (2004). The influence of coating materials on some properties of alginate beads and survivability of microencapsulated probiotic bacteria. *International Dairy Journal*, 14, 737–743.
Kumar, V., Kothari, S. H., & Banker, G. S. (2001). Compression, compaction, and disintegration properties of low crystallinity celluloses produced using different agitation rates during their regeneration from phosphoric acid solutions. *AAPS PharmSciTech.*, 2(2). Article 7.
Nussinovitch, A., & Zvitov-Marabi, R. (2008). Unique shape, surface and porosity of dried electrified alginate gels. *Food Hydrocolloids*, 22, 364–372.
Olivas, G. I., & Barbosa-Cánovas, G. V. (2008). Alginate–calcium films: Water vapor permeability and mechanical properties as affected by plasticizer and relative humidity. *Lebensmittel-Wissenschaft und-Technologie*, 41, 359–366.
Rassis, D. K., Saguy, I. S., & Nussinovitch, A. (2002). Collapse, shrinkage and structural changes in dried alginate gels containing fillers. *Food Hydrocolloids*, 16, 139–151.
Rastello De Boisseson, M., Leonard, M., Hubert, P., Marchal, P., Stequert, A., Castel, C., et al. (2004). Physical alginate hydrogels based on hydrophobic or dual hydrophobic/ionic interactions: Bead formation, structure, and stability. *Journal of Colloid and Interface Science*, 273, 131–139.
Rhim, J. (2004). Physical and mechanical properties of water resistant sodium alginate films. *Lebensmittel-Wissenschaft und-Technologie*, 37, 323–330.
Ribeiro, C. C., Barrias, C. C., & Barbosa, M. A. (2004). Calcium phosphate–alginate microspheres as enzyme delivery matrices. *Biomaterials*, 25, 4363–4373.
Rough, S. L., Wilson, D. I., Bayly, A., & York, D. (2003). Tapping characterization of high shear mixer agglomerates made with ultra-high viscosity binders. *Powder Technology*, 132, 249–266.
Sajilata, M. G., Singhal, R. S., & Kulkarni, R. (2006). Resistant starch: A review. *Comprehensive Reviews in Food Science and Food Safety*, 5, 1–17.
Schebor, C., Burin, L., Pilar Buera, M., & Chirife, J. (1999). Stability to hydrolysis and browning of trehalose, sucrose and raffinose in low-moisture systems in relation to their use as protectants of dry biomaterials. *Food Science and Technology*, 32, 481–485.
Shilpa, A., Agrawal, S. S., & Ray, A. R. (2003). Controlled delivery of drugs from alginate matrix. *Journal of Macromolecular Science Part C: Polymer Reviews*, 43, 187–221.
Skjåk-Bræk, G., Grasdalen, H., & Smidsrød, O. (1989). Inhomogeneous polysaccharide ionic gels. *Carbohydrate Polymers*, 10, 31–54.
Sriamornsak, P., Thirawong, N., Cheewatanakornkool, K., Burapapadh, W., & Sae-Ngow, W. (2007). Cryo-scanning electron microscopy (cryo-SEM) as a tool for studying the ultrastructure during bead formation by ionotropic gelation of calcium pectine. *International Journal of Pharmaceutics*, 352, 115–122.
Tal, Y., van Rijn, J., & Nussinovitch, A. (1997). Improvement of structural and mechanical properties of denitrifying alginate beads by freeze-drying. *Biotechnology Progress*, 13, 788–793.
Zohar-Perez, C., Chet, I., & Nussinovitch, A. (2004). Irregular textural features of dried alginate-filler beads. *Food Hydrocolloids*, 18, 249–258.